Deformations of the Weyl Character Formula for $SO(2n+1)$ via Ice Models

Yulia Alexandr* Patricia Commins† Alexandra Embry‡ Sylvia Frank§
Yutong Li¶ Alexander Vetter‖

August 5, 2018

Abstract

The irreducible representations of classical groups can often be encoded by Young tableaux and then explored further using combinatorial techniques. Many interesting results have been obtained for Cartan types A and C from the tableaux that describe their branching rules. The main goal of this paper is to study different types of Young tableaux that stem from various branching rules of $SO(2n+1,\mathbb{C})$ representations. In particular, we explore combinatorial properties of these tableaux and their relationship with objects known as ice models that arise in statistical mechanics. We introduce a special type of ice model, where the top row is a 5-vertex model, that is in bijection with the tableaux rules described by Sundaram and assign weights to the vertices of the resulting model that give us the deformation of the Weyl character formula for Cartan type B. We also introduce an ice model with every third row being a 3-vertex model for the tableaux rules described by Koike and Terada as well as show that there exist no ice model in bijection with tableaux described by Proctor.

1 Introduction

The mathematical framework of statistical mechanics is closely related to the theory of group representations. In particular, it involves combinatorial manifestations of the Weyl character formula. We wish to study deformations of this formula and its relationship with a type of tetravalent graphs called ice models, which can find applications in the description of many combinatorial and representation theoretical problems. Kuperberg[10] used these models to solve the problem of counting classes of alternating sign matrices. In [2], using ice models, the authors recovered deformations due to Okada [12].

The study of representations using combinatorial objects began with Tokuyama[15], who gave a deformation of the Weyl character formula in the case of $GL(n,\mathbb{C})$ through the use of strict Gelfand-Tsetlin patterns. Brubaker et al. [1] supplied an alternative proof of Tokuyama's formula using the

*Wesleyan University, CT
†Carleton College, MN
‡Indiana University, IN
§Amherst College, MA
¶Haverford College, PA
‖Villanova University, PA

Yang-Baxter Equation.

The process of translating a group's representations into ice models involves several steps. First, given some tableaux rules (which stem from branching rules of a group's representations), we aim to display a bijection between the tableaux following those rules and some Gelfand-Tsetlyn-type patterns. Then, we restrict our attention to only strict Gelfand-Tsetlin-type patterns and the corresponding shifted tableaux – purely combinatorial objects that are in bijection with them. Next, we construct an ice model that both of these objects biject with. Finally, we assign weights to the vertices in the resulting ice model such that its partition function that sums over all admissible states is equal to the product of the type B deformation formula and the character of $SO(2n+1, \mathbb{C})$. Following these steps, we obtain a fully functioning model for the tableaux first introduced by Sundaram, partial results for the tableaux described by Koike and Terada, and show that no ice model can properly describe the branching rules that Proctor tableaux encode.

2 Preliminaries

To help the reader become familiar with our study of the deformed characters of $SO(2n+1, \mathbb{C})$, we introduce the topic using the well-studied case of $GL(n, \mathbb{C})$. We first introduce the Weyl Character Formula. In order to study the deformations of this formula, we turn to the following combinatorial objects: Gelfand-Tsetlin patterns, strict Gelfand-Tsetlin patterns, semistandard Young tableaux, shifted Young tableaux, and ice models.

2.1 Weyl Character Formula

We begin with a description of an important formula for our work. Recent research involves combinatorial manifestations of the Weyl character formula. Let π be an irreducible, finite-dimensional representation of a complex semisimple Lie algebra $\mathfrak{g}$. Let $\mathfrak{h}$ be a Cartan subalgebra of $\mathfrak{g}$. Then, we can define the character of the irreducible representation $ch_\pi(H) : \mathfrak{h} \to \mathbb{C}$ by

$$ch_\pi(H) = tr(e^{\pi(H)}) \tag{1}$$

This character can be determined based upon the highest weight of π. We can define any highest weight λ and obtain the character of an irreducible representation through the Weyl Character Formula. The Weyl character formula is equivalent to:

Theorem 2.1.1 (Weyl Character Formula)**.** $ch_\pi(H) = \dfrac{\sum_{w \in W} (-1)^{l(w)} e^{w(\lambda+\rho)(H)}}{\sum_{w \in W} (-1)^{l(w)} e^{w(\rho)(H)}}$

where W is a Weyl group, ρ is the half sum of the positive roots of the corresponding root system, λ is the highest weight of the irreducible representation, and $l(w)$ is the minimal length of the Weyl group element. We wish to study deformations of this formula, which are essentially equivalent to clearing the denominator.

Theorem 2.1.2. *Weyl Character Formula for $GL(n, \mathbb{C})$*
Let $\lambda = (\lambda_n \geq \lambda_{n-1} \geq \ldots \lambda_1 \geq 0)$ index an irreducible representation of $GL(n, \mathbb{C})$ and let $s_\lambda(\mathbf{z})$ be the corresponding character, where $\mathbf{z} = (z_1, \ldots, z_n)$. Let $\rho = (n-1, n-2, \ldots, 0)$. Then, the Weyl

character formula says:

$$s_\lambda(\mathbf{z}) = \frac{\sum_{w\in S_n} sgn(w)\mathbf{z}^{w(\lambda+\rho)}}{\sum_{w\in S_n} sgn(w)\mathbf{z}^{w(\rho)}} \tag{2}$$

where $w(\mu)$ is the n-tuple from applying the permutation of w to μ.

Example 2.1.1. $n = 2$, $\lambda = (3, 1)$

$$s_\lambda(\mathbf{z}) = \frac{\sum_{w\in S_n} sgn(w)\mathbf{z}^{w(\lambda+\rho)}}{\sum_{w\in S_n} sgn(w)\mathbf{z}^{w(\rho)}} \tag{3}$$

$$s_{(3,1)}(z_1, z_2) = \frac{\sum_{w\in S_2} sgn(w)\mathbf{z}^{w(4,1)}}{\sum_{w\in S_2} sgn(w)\mathbf{z}^{w(1,0)}} \tag{4}$$

$$= \frac{\mathbf{z}^{(4,1)} - \mathbf{z}^{(1,4)}}{\mathbf{z}^{(1,0)} - \mathbf{z}^{(0,1)}} \tag{5}$$

$$= \frac{z_1^4 z_2 - z_1 z_2^4}{z_1 - z_2} \tag{6}$$

$$= z_1^3 z_2 + z_1^2 z_2^2 + z_1 z_2^3 \tag{7}$$

One of the reasons we care is because our result is always a symmetric function. It turns out, we have very nice combinatorial objects that give us the above function.

2.2 Gelfand-Tsetlin Patterns

A Gelfand-Tsetlin pattern is a triangular array of non-negative integers:

$$\begin{array}{ccccccccccc} a_{1,1} & & a_{1,2} & & \cdots & & a_{1,n-1} & & a_{1,n} \\ & a_{2,1} & & a_{2,2} & \cdots & a_{2,n-1} & & a_{2,n} & \\ & & & & \cdots & & & & \\ & & & a_{n-1,1} & & a_{n-1,2} & & & \\ & & & & a_{n,1} & & & & \end{array} \tag{8}$$

subject to:

1. $a_{i,j-1} \geq a_{i,j} \geq a_{i,j+1} \geq 0$
2. $a_{i-1,j} \geq a_{i,j} \geq a_{i-1,j+1}$

In strict Gelfand-Tsetlin patterns, we drop the equality on each side in the first condition. Thus, rows are strictly decreasing. Let $GT(\lambda)$ be the set of Gelfand-Tsetlin patterns with top row λ. Let R_i be the sum of the i^{th} row in the GT pattern. Then, we get the following result:

Theorem 2.2.1. *Let $\lambda = (\lambda_n \geq \lambda_{n-1} \geq \ldots \lambda_1 \geq 0)$, then*

$$s_\lambda(\mathbf{z}) = \sum_{P\in GT(\lambda)} \mathbf{z}^{wt(P)} \tag{9}$$

where

$$\mathbf{z}^{wt(P)} := z_1^{p_1} z_2^{p_2} \ldots z_n^{p_n} \tag{10}$$

$wt(P) := (p_1, p_2, \ldots, p_n)$, $p_i = R_i - R_{i+1}$ for $i \in \{1, \ldots, n-1\}$, and $p_n = R_n$.

Thus, we have a combinatorial interpretation for the character formula of $GL(n, \mathbb{C})$. We now examine a second combinatorial description.

2.3 Semistandard Young Tableaux

Let $\lambda = (\lambda_n \geq \lambda_{n-1} \geq \cdots \geq \lambda_1 \geq 0)$ be a partition. We fill a Young diagram of shape λ using the alphabet $1 < 2 < \cdots < n\}$ such that:

1. Rows are weakly increasing.
2. Columns are strictly increasing.

2.3.1 Bijection between Gelfand-Tsetlin Patterns and Semistandard Young Tableaux

Let $SSYT(\lambda)$ be the set of Young tableaux with shape λ. Then, we have the following result:

Theorem 2.3.1. *Let $\lambda = (\lambda_n \geq \lambda_{n-1} \geq \ldots \lambda_1 \geq 0)$ then,*

$$s_\lambda(\mathbf{z}) = \sum_{T \in SSYT} \mathbf{z}^{wt(T)} \tag{11}$$

where $\mathbf{z}^{wt(T)} = \prod_{i=1}^{n} z_i^{c(i)}$, and $c(i)$ is the number of i's in T.

We now have two different combinatorial objects that describe our characters. Also note that we have a bijection

$$SSYT(\lambda) \xleftrightarrow{1 \text{ to } 1} GT(\lambda) \tag{12}$$

To move between tableaux and Gelfand-Tsetlin patterns, we can label the rows of a Gelfand-Tsetlin from bottom to top with the letters of our alphabet for $GL(n, \mathbb{C})$. The bottom entry corresponds with the number of 1 entries in the first row of the tableaux. Each entry in the second row of the pattern corresponds to the number of entries in the first and second rows of the tableaux, respectively. You fill in the boxes of the tableaux with 2s until the tableaux boxes are filled corresponding to the length given by the pattern entries in that row. This is continued until the tableaux is of shape λ.

Example 2.3.1.

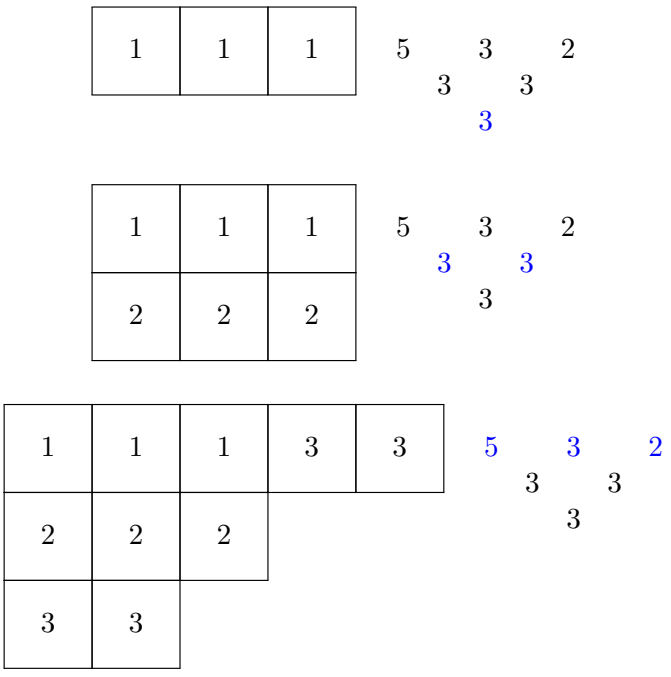

Later, we explore similar bijections for variations of Gelfand-Tsetlin patterns and Young tableaux. However, we are still not finished.

2.4 Tokuyama's Formula

Let $\lambda = (\lambda_n \geq \lambda_{n-1} \geq \cdots \geq \lambda_1 \geq 0)$ be a partition. Let $\rho = (n-1, n-2, \ldots, 0)$. Let $SGT(\lambda+\rho)$ be the set of strict Gelfand-Tsetlin patterns with top row $(\lambda+\rho)$. Let $T \in SGT(\lambda+\rho)$. Consider the tuples (a, b, c) in T such that:

$$\begin{array}{ccc} a & & b \\ & c & \end{array} \tag{13}$$

Definition 2.4.1. A **special entry** of a strict Gelfand-Tsetlin pattern is an entry c such that $a > c > b$. We define $S(T)$ to be the number of special entries.

Definition 2.4.2. A **left-leaning entry** of a strict Gelfand-Tsetlin pattern is an entry c such that $a = c$. We define $L(T)$ to be the number of left-leaning entries.

We now examine a relationship between strict Gelfand-Tsetlin patterns and the Schur polynomials.

Theorem 2.4.1 (Tokuyama's Formula [15])**.**

$$\prod_{1 \leq i < j \leq n} (z_i + t z_j) s_\lambda(\mathbf{z}) = \sum_{T \in SGT(\lambda+\rho)} (1+t)^{S(T)} t^{L(T)} \mathbf{z}^{wt(T)} \tag{14}$$

This type of formula is known as a deformed character. We now investigate certain values of t. Recall the Weyl character formula for $GL(n, \mathbb{C})$. We have that,

$$\sum_{w \in S_n} sgn(w) \mathbf{z}^{w(\rho)} = \prod_{1 \leq i < j \leq n} (z_i - z_j) \tag{15}$$

Now, if we consider Tokuyama's formula, letting $t = -1$ we get the character times the right-hand side of equation 15. Thus, we clear the denominator of the character. Further, if $t = 0$, the right side of equation 14 gives the original description of the character in terms of GT patterns. Thus, we have this new combinatorial object, strict GT patterns, that give us another variation of our formula. We have another combinatorial object in bijection with strict GT patterns.

2.5 Shifted Young Tableaux

We now create shifted tableaux in order to show a bijection with strict Gelfand-Tsetlin patterns. Let $\rho = (n-1, n-2, \ldots, 0)$. We consider a shifted Young tableaux to be of shape $\lambda+\rho$ by attaching a standard tableaux of shape ρ to the left side of the standard tableaux of shape λ. Here is an example:

2.5.1 Example

Let $\lambda = (5, 3, 2, 1)$, then the standard tableaux looks like:

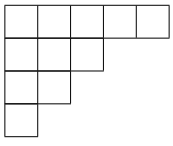

(16)

If we shift our tableaux by $\rho = (3, 2, 1, 0)$, then our new tableaux will look like:

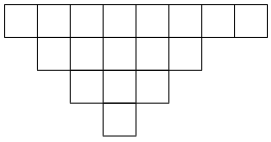

(17)

From this change, we have new rules for the filling the tableaux:

1. Rows are weakly increasing.
2. Columns are weakly increasing.
3. Diagonals are strictly increasing.

Let $SYT(\lambda + \rho)$ be the set of shifted Young tableaux that satisfy the above conditions. From these tableaux, we again have a bijectiont:

$$SYT(\lambda + \rho) \xleftrightarrow{1 \text{ to } 1} SGT(\lambda + \rho) \tag{18}$$

With all of this preliminary work, we now move on to a combinatorial object inspired by statistical physics.

2.6 Ice Models

Definition 2.6.1. An ice state is a tetravalent directed graph.

In the case of $GL(n, \mathbb{C})$, we consider an ice state admissible if and only if there are two edges pointed to and from each vertex. Let $\lambda = (\lambda_n \geq \lambda_{n-1} \geq \cdots \geq \lambda_1 \geq 0)$ be a partition. We then obtain $(\lambda + \rho)$ and form an ice state subject to the following conditions:

1. There are n rows.
2. There are $\lambda_n + n$ columns, labeled from right to left $0, 1, 2, \ldots, \lambda_n + n - 1$.
3. We label the rows from bottom to top in increasing order of the alphabet for $GL(n, \mathbb{C})$.
4. All arrows on the left-hand side point to the right.
5. All arrows on the bottom point down.
6. All arrows on the right-hand side point to the left.
7. If $i \in (\lambda + \rho)$, the column i arrow points up; otherwise it points down.

The final four conditions are our boundary conditions. We fill in the remaining edges such that every vertex has two arrows pointing in and two arrows pointing out. The admissible states of the ice models are in bijection with strict GT patterns. We can view the vertices of the ice model as points on a lattice. For $T \in SGT$, and $a_{i,j} \in T$, then the vertex in the i^{th} row from the top and in the column indexed by $a_{i,j}$ has an up arrow directly above it. The remaining column edges have down arrows. In particular, we have the bijection:

$$SGT(\lambda + \rho) \xleftrightarrow{1 \text{ to } 1} ICE(\lambda + \rho) \tag{19}$$

2.6.1 Example of Ice Boundary Conditions

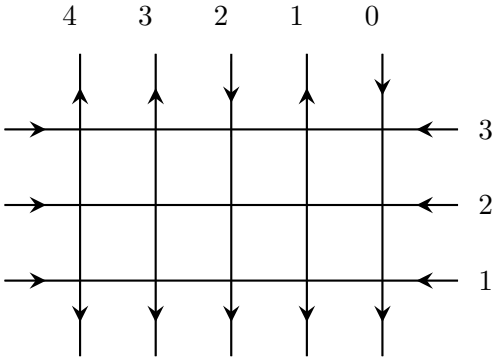

Figure 1: Ice Boundary Conditions for $\lambda + \rho = (4, 2, 1)$

2.6.2 Boltzmann Weights

Depending on the orientation of the arrows around a vertex, each vertex is assigned a particular Boltzmann weight. Invalid configurations of arrows have a Boltzmann weight of 0. The following are nonzero Boltzmann weights for the $GL(n, \mathbb{C})$ ice models as found in [1].

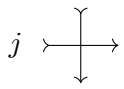	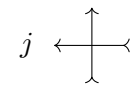	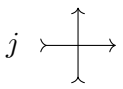	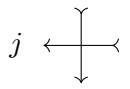	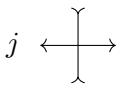	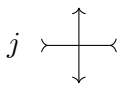
$NW = 1$	$SE = z_i$	$SW = t$	$NE = z_i$	$NS = z_i(t + 1)$	$EW = 1$

Figure 2: Boltzmann weights for each of the six valid vertex orientations

2.6.3 Partition Function on Ice Models

From this description of ice models for $GL(n, \mathbb{C})$, we define a partition function $Z(\lambda)$. Let $ICE(\lambda+\rho)$ be the set of all admissible ice models with top row $\lambda+\rho$. For a particular $\mathcal{I} \in ICE(\lambda+\rho)$, assign the Boltzmann weights as in the previous section. Let $w(\mathcal{I})$ be the product of the Boltzmann weights of each vertex in the ice model. Then, our partition function is the following:

$$Z(\lambda) = \sum_{\mathcal{I} \in ICE} w(\mathcal{I}) \tag{20}$$

The following is proved in [1]:

Theorem 2.6.1.

$$Z(\lambda) = \prod_{1 \le i < j \le n} (z_i + t z_j) s_\lambda(\mathbf{z}) \tag{21}$$

Thus, using those Boltzmann weights, we obtain Tokuyama's formula. Hence, ice models are another combinatorial object to describe our deformed character.

2.7 Our Work

The previous results are all for $GL(n, \mathbb{C})$. We follow the above process but consider the group $SO(2n+1, \mathbb{C})$. In particular, we look at three different types of tableaux due to Sundaram [14], Koike-Tarada [9], and Proctor [13]. We create variants of Gelfand-Tsetlin patterns for each of these tableaux, and then show that strict GT patterns only exist for Sundaram and Koike-Terada tableaux. These strict GT patterns also give us a bijection to ice models with new boundary conditions. In the Sundaram case, we determine Boltzmann weights that give us a deformation of the Weyl character formula for Cartan Type B. Further, we explore the origins of these tableaux through branching rules for $SO(2n+1, \mathbb{C})$.

We examine relationships between our combinatorial objects in the following way.

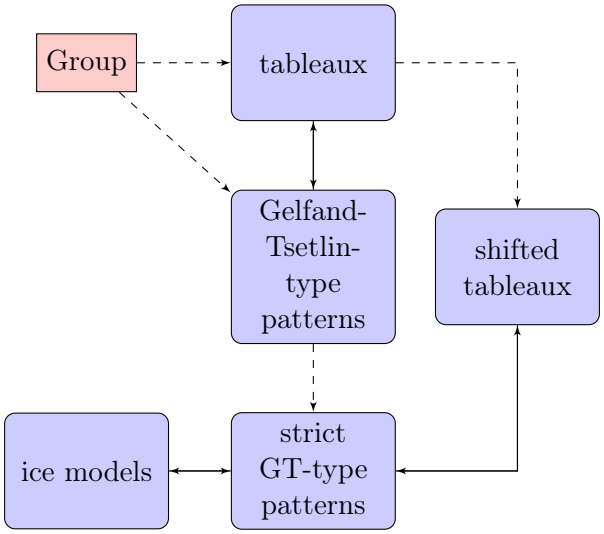

In this diagram, the black double-sided arrows represent bijections that are relatively easy to move between. The dotted arrows represent relationships that are less clear. Specifically, a group's representations' branching rules lead to a set of rules for tableaux and Gelfand-Tsetlin type patterns, but it is not clear exactly which branching rules make versions of tableaux and Gelfand-Tsetlin patterns that are easy to work with or have relationships with ice models. Further, there are relationships between tableaux and shifted tableaux as well as between Gelfand-Tsetlin -ype patterns and strict Gelfand-Tsetlin-type patterns, but they are not in bijection and the rules to move between them are less obvious and up to interpretation.

3 Sundaram Tableaux

3.1 Construction

Let $\lambda = (\lambda_n \geq \lambda_{n-1} \geq \dots \lambda_2 \geq 0)$ be a partition with n parts. Then, λ is the highest weight of an irreducible representation of $SO(2n+1)$. Further, we can find the character of this representation through the use of certain Young tableaux. Let λ define the length of the rows of such a tableaux. We fill the Young diagram with the alphabet $\{1 < \bar{1} < \cdots < n < \bar{n} < 0\}$ and the following rules:

1. Rows are weakly increasing.

2. Columns weakly increase, with strictly increasing nonzero entries.

3. No row contains multiple 0s.

4. In row i, all entries are greater than or equal to i.

We define the weight of a particular tableaux as the following:

$$\prod_{i=1}^{n} x^{w(i)-w(\bar{i})} \tag{22}$$

where $w(i)$ and $w(\bar{i})$ are the number of i and $\bar{i}$ in the Young tableaux. Sundaram shows that

$$s^{so}_{(\lambda)} = \sum_{T \in SSYT} \prod_{i=1}^{n} x^{w(i)-w(\bar{i})} \tag{23}$$

where SSYT is the set of Young diagrams filled according to the above rules, and $s^{so}_{(\lambda)}$ is the character of the irreducible representation of $SO(2n+1)$ indexed by λ. The question is, why do these tableaux exist?

3.2 Branching Rules

Polynomial representations of classical groups are parametrized by Young tableaux. We can look to the branching rules of these representations to further understand where the tableaux rules come from.

3.2.1 Relation to Sp(2n) Tableaux

The reason the Sundaram Tableaux exist for the representations of $SO(2n+1)$ is because of the following:

$$s^{so}_{\lambda} = \sum_{\mu \subseteq \lambda} s^{sp}_{(\mu)} \tag{24}$$

where $\mu = (\mu_1 \geq \mu_2 \geq \ldots \mu_{n-1} \geq \mu_n > 0)$, s^{sp}_{μ} is the character of the irreducible representation of $Sp(2n)$ indexed by μ, and $\mu \subseteq \lambda$ if and only if $\lambda_i - \mu_i \leq 1$ for all i. Further, we can construct tableaux for $Sp(2n)$ using the exact same rules as the $SO(2n+1)$ tableaux, excluding 0 in the alphabet, and this was done by King [5]. Thus, the question becomes, why do these tableaux exist for $Sp(2n)$?

3.2.2 Restriction of Sp(2n) Representations

In 1962, Zhelobenko showed the restriction $Sp(2n) \downarrow Sp(2n-2) \times U(1)$ is as follows [16]:

$$(\lambda) \downarrow = \sum_{x,y} (\lambda / x \cdot y)\{x - y\} \tag{25}$$

where x and y are one-partitions, and / and $\cdot$ are Schur function quotients and products determined by the Littlewood-Richardson rule, which is found in [8]. For our purposes λ/z means removing z boxes, no two from the same column. Further, x means the number of removals of n and y

refers to the number of removals of $\bar{n}$. The tableaux construction from King arises because the formula above implies that the n^{th} row in T_λ has a value other than n or $\bar{n}$, then that tableaux vanishes in the restriction. Hence, the fourth condition in our tableaux rules is referred to as the symplectic condition on page 3160 in [8]. From that restriction relation, Wallach and Yacobi gave an explicit branching formula. Further, Howe, Lavicka, Lee, and Soucek describe this in terms of Young diagrams, and use it in order to produce a Skew Pieri rule for $Sp(2n)$ [6].

3.3 Gelfand-Tsetlin-Type Patterns

We define a new type of Gelfand-Tsetlin pattern that we will use for our ice models. We have the following:

$$\begin{array}{ccccccccccccccc}
a_{1,1} & & a_{1,2} & & \cdots & & & & a_{1,n} & & & & 0 \\
& a_{2,1} & & a_{2,2} & & & \cdots & & & & a_{2,n} & & \\
& & a_{3,1} & & a_{3,2} & & & & \cdots & & & & a_{3,n} \\
& & & & & & \cdots & & & & & & \\
& & & & & & a_{2n-2,1} & & & & a_{2n-2,2} & & \\
& & & & & & & & a_{2n-1,1} & & & & a_{2n-1,2} \\
& & & & & & & & & & a_{2n,1} & & \\
& & & & & & & & & & & & a_{2n+1,1}
\end{array} \tag{26}$$

3.4 Shifted Tableaux and Strict Gelfand-Tsetlin-Type Patterns

In this case, our shifted tableaux rules are the following:

1. Rows are weakly increasing.
2. Columns are weakly increasing.
3. Diagonals are strictly increasing.
4. No row contains consecutive 0s.
5. The first entry in row i is either i or $\bar{i}$.

For us, we only want strict Gelfand-Tsetlin-type patterns in order to construct valid corresponding ice models. In the Sundaram case, in order to biject with the shifted tableaux, our "strict" Gelfand-Tsetlin-type patterns will include the following constraints:

1. $a_{i,j-1} > a_{i,j} > a_{i,j+1} \geq 0$
2. $a_{2k,n-k+1} \neq 0$
3. $a_{1,k} - a_{2,k} \leq 1$

The first condition, which simply means that each row in our pattern is strictly increasing, allows us to create an ice model out of these patterns. The second condition is precisely equivalent to condition 5 of our shifted tableaux. The third condition is equivalent to the fourth condition of our shifted tableaux. For us, the top row of our pattern is exactly equivalent to $\lambda + \rho$ and we add a 0 at the end for convenience.

Lemma 3.4.1. *For a given partition λ, we form the shifted tableaux of shape $\lambda + \rho$, and we let our top row of our Gelfand-Tsetlin pattern be equivalent to $\lambda + \rho$ with a 0 at the end. The permissible fillings of the shifted tableaux are in bijection with these Gelfand-Tsetlin type patterns.*

Proof. We propose an algorithm that has an inverse process as proof. First, let row 2n+1 of our Gelfand-Tsetlin type pattern correspond to filling our tableaux with 1, let row 2n correspond to filling with $\bar{1}$, and in general, let row 2k+1 correspond to n-k+1 and let row 2k correspond to $\overline{n-k+1}$ for $k \geq 1$. Finally, let row 1 of the pattern correspond to filling with 0.

Beginning from the bottom row of the Gelfand-Tsetlin type pattern, we fill out the shifted tableaux using the numbers just described, as done in the General Linear Group case. It is easy to see that constraint 2 of the strict Gelfand-Tsetlin type patterns implies that either i or $\bar{i}$ will be on the main diagonal of row i in the tableaux. This algorithm also clearly forces our rows to be weakly increasing. Further, because the rows of the Gelfand-Tsetlin pattern are strictly decreasing, our corresponding columns will be weakly increasing. Further, condition 4 ensures that we do not add two 0s to any row in the shifted tableaux. Additionally, all diagonals are strictly increasing increasing because of our strict decreasing conditions in the GT model.

Now we claim this algorithm is reversible. In particular, we can form a GT pattern from the bottom up by looking at the already filled out shifted tableaux. The conditions are clear from this process. It is also clear this algorithm produces a unique result in either direction. Thus, we have a bijection. □

3.5 Sundaram Tableaux and Ice Models

In the Sundaram case, we follow the initial ice model conditions as described in section 4. Additionally, we have the following boundary conditions:

1. The rightmost arrow of the first row always points out.
2. Further, the rows labeled with i and $\bar{i}$ are connected by a loop on the right hand side. They are either connected by an A or B loop.

3.5.1 Example

Let $\lambda = (3, 2, 0)$, and consider the following Gefland-Tsetlin-Type pattern:

$$\begin{array}{ccccccc} 3 & & 2 & & 0 \\ & 3 & & 1 & \\ & & 2 & & 1 \\ & & & 2 & \\ & & & & 1 \end{array}$$

Then, Figure 4 shows an ice model with the boundary conditions filled in. Figure 5 shows the ice model with the boundary conditions and the Gelfand-Tsetlin-Type entries filled in. Finally, Figure 6 shows the fully filled-in ice model.

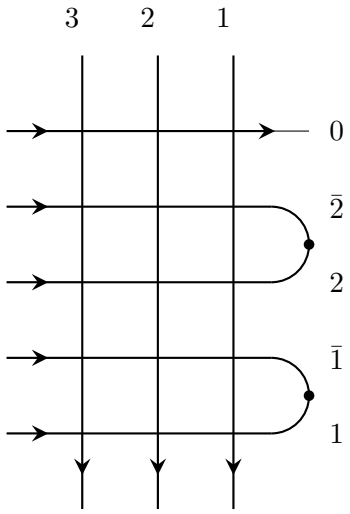

Figure 3

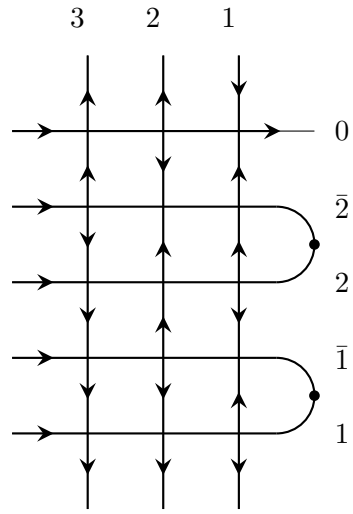

Figure 4

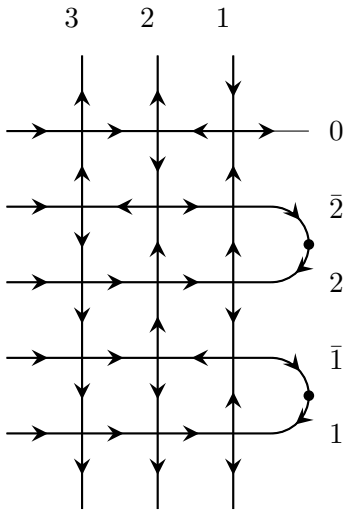

Figure 5

Lemma 3.5.1. *If $a_{2k+1,n-k+1} = 0$, then the loop between the rows indexed by $n-k+1$ and $\overline{n-k+1}$ goes counterclockwise. If not, then the loop goes clockwise. Further, in row 0, the arrow points out.*

Proof. We begin by proving the latter statement. Suppose instead of loops on the right side of our ice model, we create a new model where we include a column labeled 0. Let (x, y) denote the vertex of the ice model in column x and row y . First, because of our convention that the first row of the Gelfand-Tsetlin type pattern ends in 0, the the vertical arrow above the vertex $(0, 1)$ points up. Because of the second constraint on strict Gelfand-Tsetlin type patterns, the vertical arrow below vertex $(0, 1)$ points out. Thus, vertex $(0, 1)$ has two edges pointed out, and the other two arrows must point towards the vertex. Hence, in row 0, the far right arrow points out.

We now prove the first statement of the lemma. We make use of Lemma 2 in section 4 from a paper by Brubaker, Bump, and Friedberg [1]. From this lemma, we get that, excluding the first row, the rightmost arrows (in the 0 column) must alternate in our model. Now we need to determine the edge above the $(2(n-k+1)+1, 0)$ vertex. Because of constraint 2 on strict Gelfand-Tsetlin type patterns, the edge below this vertex points away. By the edge to the right of the vertex points in. Thus, if $a_{2k+1,n-k+1} = 0$ in our GT pattern, then the arrow pointing above the $(2(n-k+1)+1, 0)$ vertex points up, and hence, the edge to the left of the $(2(n-k+1)+1, 0)$ vertex points towards it. Further, the edge to the left of the $(2(n-k+1), 0)$ vertex points away from the vertex. Hence, our loop will be counterclockwise. The argument uses the same reasoning if $a_{2k+1,n-k+1} \neq 0$. □

We use the following convention. We consider the state of a vertex to be either $\{NE, NS, NW, EW, SE, SW\}$, where the state is determined by which arrows pointed in towards the vertex. In particular, if the top edge points in and the right edge points in at a vertex, then we label it with NE.

Lemma 3.5.2. *No vertex in the top row has a state of NE if and only if the fourth condition of the Gelfand-Tsetlin Patterns is satisfied.*

Proof. First, suppose, toward a contradiction, that there exists a vertex with a NE state in the top row. In particular, this cannot be the top left vertex because the top left vertex always points from the West. Further, let us assume this is the left most NE vertex. Thus, the next vertex over must have top edge pointing away from the vertex. Now, if this is an EW state, then we have a contradiction, since the arrow pointing up on the top edge corresponds to an element λ_k of our initial partition. Further, condition 4 on our GT patterns imply that either λ_k or $\lambda_k - 1$ must appear in our second row of the GT pattern. Thus, the vertex next to NE must be a SE vertex. Suppose the next vertex is a EW vertex. Again we have a contradiction, because we have $\lambda_k + 1$ and λ_k appearing in our initial partition. Thus, at least two of $\lambda_k + 1$, λ_k, and $\lambda_k - 1$ must appear in the second row, but this is not the case. Thus, we must have another SE vertex. Thus suppose we have j SE vertices to the left of the NE vertex, and because of the construction, eventually we must get a vertex with EW vertex as the left side of our model points in. In this case, we have j+1 consecutive arrows pointing out on the top edges. However, we only have j arrows pointing up from the vertices of the second row. Thus, there exists an element in our GT pattern such that $a_{1,k} - a_{2,k} \not\leq 1$. Then this vertex must have an EW configuration and the vertex to its right must be EW.

For the other direction, suppose, toward a contradiction, that the fourth rule is violated. Let $\alpha_1, ..., \alpha_n$ denote the spots where the arrows point up in a row and $\beta_1, ..., \beta_m$ denote the spots where the arrows point up in the row below it. Then there exists some α_i and β_i such that $\alpha_i > \beta_i + 1$. So we have the situation where the EW and NE configurations are forced and we obtain the desired contradiction. □

4 Koike-Terada Tableaux

4.1 Construction

Another set of tableaux rules for the $SO(2n+1)$ group is defined by Koike and Terada in [9].

Given a partition $\lambda = (\lambda_n \geq \lambda_{n-1} \geq \cdots \geq \lambda_1 \geq 0)$, we fill a standard Young tableau of shape λ with the alphabet $\{1 < \bar{1} < \bar{\bar{1}} < 2 < \bar{2} < \bar{\bar{2}} \cdots n < \bar{n} < \bar{\bar{n}}\}$. Let $T_{i,j}$ be the entry of the tableau in the i-th row and the j-th column. The filling of the tableau must satisfy the following conditions:

1. k can only appear in $T_{k,1}$
2. Rows are weakly increasing
3. Columns are strictly increasing
4. $T_{i,j} \geq i$

Given a tableau filled according to these rules, the weight of the tableau is consequently defined.

Definition 4.1.1. Let T be a tableau of shape λ. The **weight** of T is the vector of integers $wt(T) = (d_1, d_2, \ldots, d_n)$, where $d_i = w(\bar{i}) - w(\bar{\bar{i}})$ denotes the difference between the number of $\bar{i}$'s and $\bar{\bar{i}}$'s in T.

We let $\mathbf{z}^{wt(T)} = z_1^{d_1} z_2^{d_2} \cdots z_n^{d_n}$. Then, summing over all tableaux of shape λ yields the character formula.

4.2 Young-Diagrammatic Description of Branching Rules

Koike and Terada gave a description of the restriction rules of representations of $SO(2n+1, \mathbb{C})$ using these tableaux. Instead of using the Gelfand-Tsetlin bases of representation spaces as in Zhelobenko [16], the tableaux rules given above directly determine the weights and multiplicities in an irreducible representation of the special orthogonal group.

Let λ be a partition. The length of λ is the number of non-zero terms and is denoted by $l(\lambda)$. A subpartition $\lambda \supset \mu = (\mu_n, \mu_{n-1}, \ldots, \mu_n - m + 1)$ is a partition of length $m \leq n$ such that $\mu_i \leq \lambda_i$, for all $n - m \leq i \leq n$. In other words, the Young diagram of λ contains the diagram of μ. The skew diagram is the set-theoretic difference $\theta = \lambda - \mu$. [11]

Under the restriction rule $SO(2n+1) \downarrow SO(2n-1) \times GL(1)$, the character of the irreducible representation parametrized by λ is related to the tableaux as follows:

$$\chi_{\lambda_{SO(2n+1)}} \downarrow SO(2n-2k+1) \times \overbrace{GL(1) \times \cdots \times GL(1)}^{k \text{ times}} = \sum_{\substack{\mu \subset \lambda, l(\mu) \leq n-k \\ T_{\lambda-\mu}}} \chi_{\mu_{SO(2n-2k+1)}} \cdot z^{wt(T)}, \quad (27)$$

where the summation runs over all possible fillings of skew tableaux of $\lambda - \mu$.

In lieu of proving Equation 27, which can be done inductively, we look at the case of $k = 1$, i.e. branching down one level. Each skew tableau gives rise to a monomial in z_n, hence the character of a representation of $GL(1)$. The tableaux of shape λ thus illustrate how a polynomial representation of $SO(2n+1)$ decomposes as a direct sum of irreducible representations of its subgroups upon restriction to $SO(2n-1) \times GL(1)$. Although this description of restriction rules is independent of Gelfand-Tsetlin bases, we shall develop an analogue of such patterns in the next section.

4.3 Gelfand-Tsetlin-Type Patterns

We developed Gelfand-Tsetlin-type patterns in bijection with the Koike-Terada tableaux. Let $a_{i,j}$ be the entry of the pattern in the i-th row and the j-th column. Given a partition $\lambda = (\lambda_n \geq \lambda_{n-1} \geq \cdots \geq \lambda_1 \geq 0)$, we create a pattern with top row λ satisfying the following rules:

1. The pattern has $3n$ rows. We will label these rows $1, \bar{1}, \bar{\bar{1}}, \cdots, n, \bar{n}, \bar{\bar{n}}$, starting from the bottom of the pattern.
2. Rows $i, \bar{i}$, and $\bar{\bar{i}}$ must have i entries that weakly decrease across the row.
3. Each entry b must be in the interval $[a, c]$, where a is the entry above and to the right of b, and c is the entry above and to the left of b.
4. Row i must end in a 1 or a 0 (for $i \in \{1, \cdots, n\}$)
5. Each entry in row $\bar{\bar{i}}$ (for $\bar{\bar{i}} \in \{\bar{\bar{1}}, \cdots, \overline{\overline{n-1}}\}$) must be left-leaning.

Rules 4 and 5 account for the first tableaux rule.
The correspondence between the Koike-Terada tableuax and Gelfand-Tsetlin-type patterns works in the same way as in the Sundaram case.

Example 4.3.1. The Gelfand Tsetlin-type pattern

$$\begin{array}{ccccccccc} 5 & & 3 & & & & & & \\ & 4 & & & 2 & & & & \\ & & 2 & & & & 1 & & \\ & & & & 2 & & & & \\ & & & & & & 1 & & \\ & & & & & & & & 0 \end{array} \tag{28}$$

corresponds with the tableau

$\overline{1}$	$\overline{\overline{1}}$	$\overline{2}$	$\overline{2}$	$\overline{\overline{2}}$
2	$\overline{2}$	$\overline{\overline{2}}$		

4.4 Shifted Tableaux and Strict Gelfand-Tsetlin-type patterns

Just like in the previous section, we would like to define a bijection between shifted tableaux and strict Gelfand-Tsetlin-type patterns to construct corresponding ice models. We will refer to a Gelfand-Tsetlin-type pattern as strict if each row is strictly increasing from right to left. Then the shifted tableaux rules are defined as follows:

1. Rows are weakly increasing.
2. Columns are weakly increasing.
3. Diagonals are strictly increasing.
4. The first entry in row k is k, $\overline{k}$ or $\overline{\overline{k}}$.

We would like to note that violation of the fifth rule would result in the following configuration in the Gelfand-Tsetlin-type pattern (thus contradicting its strictness):

$$\begin{array}{ccccccccc} c & & 0 & & 0 & & & & \\ & c & & 0 & & & & & \\ & & c & & 0 & & & & \\ & & & c & & & 0 & & \\ & & & & c & & & & \\ & & & & & & b & & \\ & & & & & & & & a \end{array} \tag{29}$$

4.5 Ice Model

The next step in the characterization of Koike-Terrada tableaux is to construct an ice model in bijection with strict patterns.
We will define our ice model to be a grid with $3n$ horizontal and λ_n vertical lines. The horizontal

lines are labeled from 1 to $\overline{\overline{n}}$ starting from the bottom and the vertical lines are labeled 1 to λ_n starting from the right. The shape and boundary conditions are given as follows:
We will allow the three possible "bends" on the right boundary of each model connecting the rows labeled $\overline{\overline{k}}$ and $\overline{k}$ for each $k \in \{1, \cdots, n\}$:

Note that the loop of the type  is not possible, as it would require having two consecutive NS configurations in the same column, which clearly can't happen. We will also allow the three possible configurations called "ties" on the right boundary of each row labeled $k \in \{1, \cdots, n\}$:

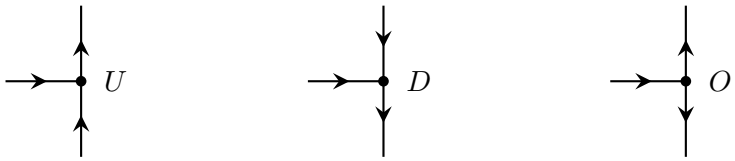

Furthermore, every row labeled $k \in \{1, \cdots, n\}$ is a three-vertex model: the only vertex configurations are SW, NW, and NE.

The next three figures demonstrate boundary conditions and the full ice model for one of the patterns of $\lambda = (2, 1)$.

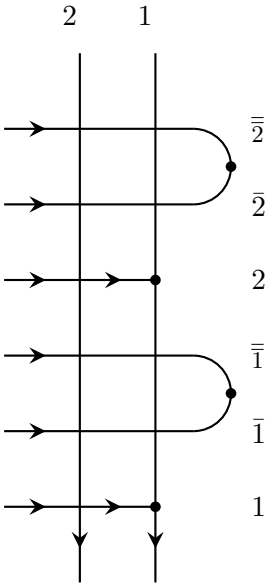

Figure 6: Boundary

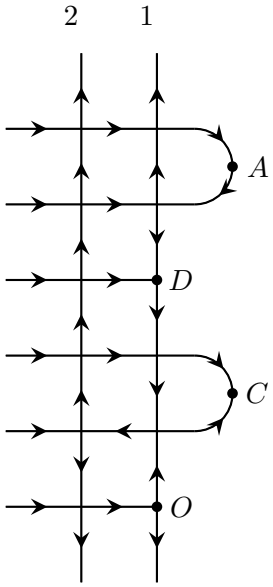

Figure 7: Ice Model

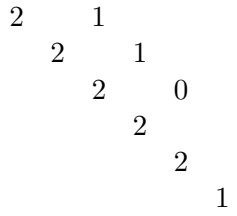

Figure 8: GT pattern

We will prove that such ice models are in bijection with strict Gelfand-Tsetlin-like patterns in the next two theorems. We will note that the first three Gelfand-Tsetlin-type pattern rules are automatically satisfied as in previous sections. It remains to prove the bijection between the strict Gelfand-Tsetlin-type patterns and the ice, which we will do with the following theorem:

Theorem 4.5.1. *The following are equivalent:*

1. *Koike-Terada Gelfand-Tsetlin-type pattern rules 4 and 5 are satisfied.*
2. *Each ice row labeled $k \in \{1, \cdots, n\}$ has no NS, SE, or EW configurations, and tie boundary conditions are satsified.*

Proof. We'll show the two directions:

(1) $\implies$ (2) First, suppose that rules 4 and 5 are satisfied. Then clearly NS isn't possible in rows labeled k, since all the entries in row $\overline{\overline{k-1}}$ are left-leaning. Now assume, toward a contradiction, that we have a SE configuration in a row labeled k. Then the configuration to the left of it is either SE again, or NE, or EW. If it is SE or NE, we look at the configuration to the left of it. We may now assume we reached the leftmost SE or NE configuration, then the state to the left must be EW because of the left boundary conditions. But this is a contradiction to rule 5, since we get a non-left-leaning entry, as the up-arrow in the EW configuration is not the rightmost in that row.

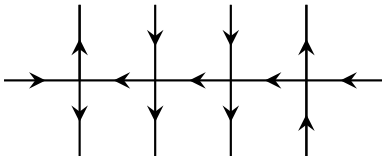

Figure 9: SE forces EW

Now we note that rule 4 directly implies that we cannot have EW in any row labeled $k \in \{1, ..., n\}$. A Gelfand-Tsetlin-type pattern row ending in 0 or 1 implies that we could only have EW in the (imaginary) 0^{th} or 1^{st} row, and none of these are possible.

We will now show that the tie boundary conditions are also implied by rules 4 and 5. So, row k must end in a 0 or a 1. If row k ends in a 1, then a 1 cannot appear in row $\overline{\overline{k-1}}$ since each entry in row $\overline{\overline{k-1}}$ must be left-leaning and strictly decreasing. This would correspond to having an EW in column 1 of our ice model if we had a full column 1, but now corresponds to the O-tie. If row k ends in a 0, then for similar reasoning we would have an EW in the 0^{th} column of our ice model, if we were to have a 0^{th} column. As stated earlier, we know SE and NS cannot appear in this row, and it is clear that neither EW nor NE can appear directy to the left of an EW. Thus, the only possible fillings for the vertex in the 1^{st} column would be a SW or a NW. Having a SW implies having the U tie boundary, and having a NW implies the D tie boundary.

(2) $\implies$ (1) First, suppose each non-bar row has no NS, SE, and EW. Then, the only vertices in the row can be NW, SW, and NE. Each of these types of vertices have the two vertical arrows pointing in the same direction, meaning the row

below it is left leaning. Thus, rule 5 is satisfied. Next, suppose the tie boundary conditions are also satisfied. Then assume, toward a contradiction, that row $k \in \{1, \cdots, n\}$ ends in a number greater than 1. This means the only possible tie configuration for row k would be D. If this is the case, all the horizontal arrows to the left of it must point right to avoid NS. However, since row k in the Gelfand-Tsetlin-type pattern has one more entry than row $\overline{\overline{k-1}}$, then eventually we will have a configuration where two consecutive vertical arrows in that row point away from each other, thus obtaining the desired contradiction, and rule 4 is satisfied.

□

5 Proctor Tableaux

5.1 Construction

We will examine one more tableaux associated to $SO(2n+1)$, as defined by Proctor.Let $\lambda = (\lambda_n \geq \lambda_{n-1} \geq \cdots \geq \lambda_1 \geq 1)$ be a partition. We fill a standard Young Tableaux of shape λ with alphabet and ordering $\{1 < 2 < \cdots < 2n < 0\}$, where 0 is infinity. We define $T_{i,j}$ to be the entry in a tableaux T in row i and column j. We fill the tableaux such that:

1. Rows are weakly increasing.
2. Columns are strictly increasing.
3. Follows the 2c orthogonal condition
4. Follows the $2m$ protection condition

Definition 5.1.1. The **2c orthogonal condition** is satisfied if for every $c \leq n$, there are less than or equal to 2c entries that are less than or equal to 2c in the first two columns, not including a 0 entry.

Definition 5.1.2. The **2m protection condition** is satisfied if for every $m \leq n$:

- If an entry in the first column is equal to 2m-1, then define i to be equal to the row number of said entry.
- Then, define k to be equal to 2m-i.
- If there is an entry in the kth row equal to 2m, let h be equal to the column number of the leftmost 2m entry.
- Then, for any j such that $2 \leq j \leq h$, $T_{k,j}$ must be equal to 2m-1. Additionally, $T_{k-1,h}$ must equal to 2m-1.
- If the suppositions do not hold for m, then the condition is trivially satisfied.

For example, if our tableaux looked like the following:

$$\begin{array}{|c|c|c|c|}\hline 1 & 1 & x & 5 \\ \hline 3 & x & 4 \\ \cline{1-3} 5 \\ \cline{1-1} \end{array} \tag{30}$$

Then to satisfy the $2m$ protection condition, every entry where there is an x (i.e. $T_{1,3}$ and $T_{2,2}$) must equal 3. If our tableaux looked like the following:

$$\begin{array}{|c|c|c|c|}\hline 1 & 1 & 3 & 5 \\ \hline x & 3 & 4 \\ \cline{1-3} 5 \\ \cline{1-1} \end{array} \tag{31}$$

Then the entry $T_{2,1}$ must be greater than or equal to 3 in order to satisfy the 2c orthogonal rule (and, in this case, it must be 3 so that the 2nd row is weakly increasing). If $T_{2,1}$ were equal to 2, then when c=1, there would be more than 2c entries in the first two columns that are less than or equal to 2c. The following tableaux satisfies all of the rules of a valid Proctor tableaux:

$$\begin{array}{|c|c|c|c|}\hline 1 & 1 & 3 & 5 \\ \hline 3 & 3 & 4 \\ \cline{1-3} 5 \\ \cline{1-1} \end{array} \tag{32}$$

5.2 Branching Rules

We have that the indexing set for these two point-wise equal sets of positive tensor orthogonal characters coincide for all n for $SO(2n+1)$ and O_{2n+1}. The rules for Proctor's tableaux are a consequence of the branching restriction $O_{2n+1} \downarrow O_{2n-1} \bigotimes O_2$ at each step, where the restriction to O_{2n-1} gives us the Protection Condition and the restriction to O_2 gives us the Orthogonal Condition. Proctor gives the following proposition.

Proposition 5.2.1. *Proctor 10.3 Let $G_N = O_N$, and let λ respectively be an N-orthogonal partition. Then the representation $G_N(\lambda)$ restricts to $\bigoplus G_{N-2}(v) \bigotimes G_2(\lambda - v)$, where the sum is over all $v \subseteq \lambda$ which are possible indexing partitions for representations of G_{N-2} such that $\lambda - v$ does not have more than 2 boxes in a column.*

5.3 Proctor Tableaux and Gelfand-Tsetlin-Type Patterns

To create Gelfand-Tsetlin-type patterns to correspond with the odd special orthogonal tableaux rules given by Proctor, we must take into consideration the effect of the 2c orthogonal condition and the 2m protection condition. We begin with our top row entries being equal to λ. The top n rows will have n entries. The n+1st row will have n-1 entries, the n+2nd row will have n-2 entries, etc, and the bottom row will have 1 entry.

To biject with the 2m protection condition, we use the following rules in our patterns.

- In order to check the following rules, all of the rows in our Gelfand-Tsetlin-type patterns must have n entries. We add 0s to the ends of our rows that have less than n entries such that each row now has n entries (including the added 0's). Additionally, we add a "0th row" at the bottom of our Gelfand-Tsetlin-type pattern that is made of n 0's.

- If there is a non-left-leaning 0 entry in an even row, we define m and i so that $a_{2m-2,i} = 0$.
- Then, define j = 2m-i.
- We check to see if $a_{2m,j} \geq a_{2m-1,j}$. If it is, we check the following:
  - $a_{2m-1,j-1} \geq a_{2m-2,j-1}$.
  - $a_{2m-1,j-1} \geq a_{2m,j}$
  - $a_{2m-2,j} \leq 1$

To biject with the $2c$ orthogonal condition, we have a restriction on the entries in an even row, $2c$. For entries in the $2c$ row, let the orthogonal sum be the sum of the entries such that for $1 \leq k \leq n$, $a_{2c,k} = a_{2c,k}$ for $a_{2c,k} \leq 2$ and $a_{2c,k} = 2$ for $a_{2c,k} > 2$. This sum must be less than or equal to $2c$.

5.4 Proctor Tableaux and Ice

Using the above restrictions on Gelfand-Tsetlin-type patterns, it can be shown that corresponding ice models do not follow naturally. In the Sundaram and Koike-Terrada bijections to ice, only Gelfand-Tsetlin-type patterns that are strictly decreasing across rows have corresponding ice models. Non-strict Gelfand-Tsetlin-type patterns do not have corresponding statistical mechanical meaning in the form of ice models. In the case of $n = 4$, we can look at the fourth row. The smallest possible strict configuration would be $\lambda_4 = 3, 2, 1, 0$. However, the orthogonal sum of that row, according to the orthogonal restrictions on Gelfand-Tsetlin-type patterns, is 5, which is greater than 4, thus breaking the restriction. Therefore, in the case of $n = 4$, there are no strict Gelfand-Tsetlin-type patterns, and consequently no valid ice models.

6 Deformation Formula for the Sundaram Case

Consider the ice models created in the Nathan Gray paper. Use the weights as he defines them. There is a bijection between his ice models and the alternating left boundary ice models found in Ivanov. Then, we have the following result:

Theorem 6.0.1. *Let $\lambda = (\lambda_n \geq \lambda_{n-1}, \geq \ldots, \geq \lambda_1 > 0)$ be a partition. Let $\rho = (n, n-1, \ldots, 2, 1)$. Let us create our ice models for $(\lambda + \rho)$ using our Gelfand-Tsetlin-type pattern rules from the Sundaram case. Using the Boltzmann weights as defined in Gray, let $\mathcal{Z}(\lambda)$ be the partition function defined on our ice states from the Sundaram case with top row $(\lambda + \rho)$. Let $C^* = \mathbf{z}^{-\rho} \prod_{i=1}^{n}(1 + tz_i^2) \prod_{i<j}(1 + tz_iz_j)(1 + z_iz_j^{-1})$, where $\mathbf{z}^{-\rho} = z_1^{-n} z_2^{-n+1} \ldots z_n^{-1}$. Let s_λ^{so} be the character of the irreducible representation of $SO(2n+1)$ indexed by λ. Then, $\mathcal{Z}(\lambda) = C^* s_\lambda^{so}$.*

Proof. Using Ivanov and Gray, for top row $(\lambda + \rho)$ in the U-turn ice models, we have the partition function $\mathcal{Z}(\lambda) = C^* s_\lambda^{sp}$, where s_λ^{sp} is the character of the irreducible representation of $Sp(2n)$ indexed by λ. Now, in our ice models, every top row has a product equal to 1. Thus, eliminating this top row, we have an ice model exactly like those in Gray, where the top row is exactly the second row of our GT pattern. Thus, let $(\lambda^{'} + \rho)$ be the second row of our GT pattern. Note that $|(\lambda + \rho)| = |(\lambda^{'} + \rho)|$ by construction of our ice models. Also note that if $\lambda_1 > \lambda_1^{'}$, the difference is exactly 1. Also, this implies every vertex in the first column of our ice models with top row $(\lambda^{'} + \rho)$ is NW, which is a

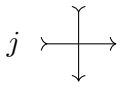	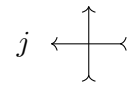	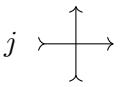	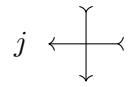	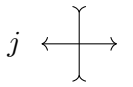	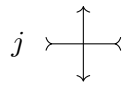 Δ Ice
1	tz_i	1	z_i	$z_i(t+1)$	1
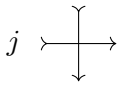	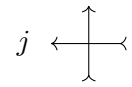	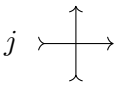	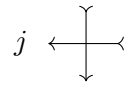	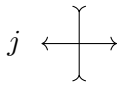	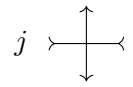 Γ Ice
1	z_i^{-1}	t	z_i^{-1}	$z_i^{-1}(t+1)$	1

Figure 10: Boltzmann weights for Δ and Γ Sundaram Ice

Figure 11: Boltzmann Weights for Sundaram Bends

weight of 1. Thus, for any given top row $(\lambda' + \rho)$, we get $\mathcal{Z}(\lambda') = C^* s^{sp}_{\lambda'}$. Thus, if we consider all possible allowed second rows of our GT patterns, we get the following:

$$\mathcal{Z}(\lambda) = \sum_{\mu \subseteq \lambda} C^* s^{sp}_{\mu} \tag{33}$$

where $\mu \subseteq \lambda$ if it is an allowed second row in our GT model. However, as a result of Sundaram,

$$\sum_{\mu \subseteq \lambda} s^{sp}_{\mu} = s^{so}_{\lambda} \tag{34}$$

Thus, in particular, we get $\mathcal{Z}(\lambda) = C^* s^{so}_{\lambda}$ □

Now we are interested in a type B character deformation times a type B character. Through an adjustment of weights from Gray, we get the following.

Corollary 6.0.1. *There exists a set of Boltzmann weights for ice models in the Sundaram case such that the partition function defined from our ice models is precisely:*

$$\mathcal{Z}(\lambda) = \prod_{i=1}^{n}(1+tz_i)\prod_{i<j}(1+tz_iz_j)(1+z_iz_j^{-1})s^{so}_{\lambda} \tag{35}$$

Proof. Consider Theorem 1. Using the weights from Gray, we make the following modification: let A_i and B_i be the clockwise and counterclockwise oriented U-turn boundary connecting row i and $\bar{i}$, respectively. We note that either A_i or B_i occurs in every ice state. Thus, let us multiply our weights for A_i and B_i by $z_i^{-n+i-1}\dfrac{(1+tz_i)}{(1+tz_i^2)}$. Thus, this means for a given ice state, we are multiplying the weight of the model by $\mathbf{z}^{-\rho}\dfrac{\prod_{i=1}^{n}(1+tz_i)}{\prod_{i=1}^{n}(1+tz_i^2)}$. Since this happens for all our ice states, we are simply

multiplying our partition function that we got from Theorem 1, by $\mathbf{z}^{-\rho}\frac{\prod_{i=1}^{n}(1+tz_i)}{\prod_{i=1}^{n}(1+tz_i^2)}$, giving the result. □

7 Concluding Remarks

Now that we have a deformation formula and corresponding ice models for Cartan type B, the question is: how "good" are our weights? It turns out that the ice models appear in special analytic L-functions. In particular, when considering Fourier expansion, the weights of the ice models are precisely the coefficients in the expansion. Thus, the next step would be to turn towards number theory to see the usefulness of our results. Further, we still have other ice models that could be assigned weights. Koike-Tarada tableaux rules produce valid statistical mechanical ice models. Thus, determining weights for these ice models and producing a type B Weyl character deformation would be useful. It seems ice models for Cartan type B are relatively unexplored compared to those of Cartan type A and C. We note that there does not seem to be any research on ice models for Cartan type D. Thus, a potential future research direction is considering the type D case.

8 Acknowledgements

This research was conducted at the 2018 University of Minnesota-Twin Cities REU in Algebraic Combinatorics. Our research was supported by NSF RTG grant DMS-1745638. We thank Benjamin Brubaker and Katherine Weber for their advice and support during our time in the Twin Cities. We also thank Jiyang Gao for his contributions to the project.

References

[1] Ben Brubaker, Daniel Bump, and Solomon Friedberg. "Schur Polynomials and The Yang-Baxter Equation". en. In: *Communications in Mathematical Physics* 308.2 (Dec. 2011), pp. 281–301.

[2] Ben Brubaker and Andrew Schultz. "The six-vertex model and deformations of the Weyl character formula". en. In: *Journal of Algebraic Combinatorics* 42.4 (Dec. 2015), pp. 917–958.

[3] Markus Fulmek and Christian Krattenthaler. "A bijection between Proctor's and Sundaram's odd orthogonal tableaux". In: *Discrete Mathematics* 161.1 (1996), pp. 101 –120.

[4] Nathan Gray. "Metaplectic Ice for Cartan Type C". PhD thesis. Sept. 2017.

[5] A.M. Hamel and R.C. King. "Symplectic Shifted Tableaux and Deformations of Weyl's Denominator Formula for sp(2n)". In: *Journal of Algebraic Combinatorics* 16.3 (Nov. 2002), pp. 269–300.

[6] Roger Howe et al. "A reciprocity law and the skew Pieri rule for the symplectic group". In: *Journal of Mathematical Physics* 58 (Nov. 2016).

[7] Dmitriy Ivanov. "Part I, Symplectic ice, Part II, Global and local Kubota symbols". PhD thesis. Aug. 2010.

[8] R.C. King and N.G.I. El-Sharkaway. "Standard Young tableaux and weight multiplicities of the classical Lie groups". In: *Journal of Physics A: Mathematical and General* 16.14 (1983), p. 3153.

[9] Kazuhiko Koike and Itaru Terada. "Young diagrammatic methods for the restriction of representations of complex classical Lie groups to reductive subgroups of maximal rank". en. In: *Advances in Mathematics* 79.1 (Jan. 1990), pp. 104–135.

[10] Greg Kuperberg. "Symmetry Classes of Alternating-Sign Matrices under One Roof". In: *The Annals of Mathematics* 156.3 (Nov. 2002), p. 835.

[11] I. G. Macdonald. *Symmetric functions and Hall polynomials*. Reprinted in paperback. Oxford classic texts in the physical sciences. Oxford: Clarendon Press, 2015.

[12] Soichi Okada. "Alternating Sign Matrices and Some Deformations of Weyl's Denominator Formulas". In: *Journal of Algebraic Combinatorics* 2.2 (1993), pp. 155–176.

[13] R.A. Proctor. "Young Tableaux, Gelfand Patterns, and Branching Rules for Classical Groups". en. In: *Journal of Algebra* 164.2 (Mar. 1994), pp. 299–360.

[14] Sheila Sundaram. "Orthogonal tableaux and an insertion algorithm for SO(2n + 1)". In: *Journal of Combinatorial Theory, Series A* 53.2 (Mar. 1990), pp. 239–256.

[15] Takeshi Tokuyama. "A generating function of strict Gelfand patterns and some formulas on characters of general linear groups". en. In: *Journal of the Mathematical Society of Japan* 40.4 (Oct. 1988), pp. 671–685.

[16] D P Zhelobenko. "The Classical Groups. Spectral Analysis of Their Finite-Dimensional Representations". In: *Russian Mathematical Surveys* 17.1 (Feb. 1962), pp. 1–94.